Operational Oceanography, Implementation at the European and Regional Scales, Proceedings of the second international Conference on EuroGOOS 11-13 March 1999, Rome, Italy, edited by N. C. Flemming et al., pp. 405-419, Elsevier Science Ltd, 2002. (Elsevier Oceanography Series, 66). ISBN: 0-444-50391-9

Multi-sensor satellite monitoring of ocean climate

T. H. Guymer[a], P. G. Challenor[a], P. Cipollini[a], D. Cromwell[a], G. D. Quartly[a], M. A, Srokosz[a] and P. D. Cotton[b]

[a]Southampton Oceanography Centre, Empress Dock, Southampton, SO14 3ZH, United Kingdom

[b]Satellite Observing Systems, 15 Church Street, Godalming, Surrey, GU7 1EL, United Kingdom

In the 20 years since Seasat demonstrated that several ocean parameters could be measured to useful accuracy from a single platform satellite oceanography has advanced significantly. Not only has it been possible to measure new parameters but the ability to undertake global monitoring for a decade or so has given new insights to some phenomena which could not have been obtained from in situ data alone.

The three examples discussed in this presentation, which have all been pioneered at SOC, have been chosen because of their relevance to climate change: variations in wave climate, the propagation of planetary waves across ocean basins and a new rainfall climatology. In addition to their use for monitoring changes in the coupled ocean-atmosphere system these datasets are invaluable for testing the models being developed for climate prediction.

Wave height can be measured as accurately from satellite altimeters as from surface buoys and data accumulated since 1985 have been used to show both that the NE Atlantic became rougher and that fluctuations in different oceans may be linked. Planetary waves are an important mechanism for carrying information across ocean basins and may modify currents such as the Gulf Stream and Kuroshio. Detection of one type (Rossby waves) from satellite measurements of sea level, sea temperature and ocean colour will be presented; the inferred characteristics have already led to revisions of standard theories with implications for the way the oceans affect climate. Although unforeseen when the sensors were designed altimeters can also be used to identify rain events. A new precipitation climatology, derived from measured backscatter intensity, will be described and compared with previous work. It has the advantage of using a single sensor-type for tropical to polar latitudes.

1. INTRODUCTION

Seasat, the first satellite dedicated to oceanography, the Advanced Very High Resolution Radiometer and the Coastal Zone Colour Scanner, all launched in 1978, clearly demonstrated that a variety of oceanographic parameters could be estimated from space. Since that time much effort has been expended in improving both the accuracy of sensors and the retrieval algorithms necessary to generate oceanic parameters from the raw data. Indeed, in a few cases the satellite sensor can now provide data more accurately and reliably than an in situ instrument (e.g. significant wave height from radar altimeters). It is also evident that

spaceborne sensors can provide global coverage at a spatial resolution which is beyond the capability of any in-water system which can be envisaged in the foreseeable future.

For some variables we now have comparatively long records (nearly 20 years for infra-red sea surface temperature (SST) and nearly 15 for altimetry) and the analysis of these is adding significantly to our knowledge by confirming and extending what had already been learnt from in situ datasets and, in some cases, through the discovery of new features.

In this paper we review some of the research into seasonal and interannual variations of the ocean carried out at Southampton Oceanography Centre which is relevant to operational oceanography. We have chosen to focus on three applications mainly using satellite altimetry, some of which were pioneered at SOC. They are: large-scale changes in wave climate, the propagation of Rossby waves across ocean basins, and a new precipitation climatology. From these we draw out key issues relating to operational oceanography and present them in the final section.

2. CHANGES IN WAVE CLIMATE

2.1. Background

Analysis of longterm, wave records from in situ platforms to the west of the UK by Bacon and Carter (1991) showed an increase in average wave height of more than 1% per year between the 1960s and 1980s. Such an increase has been confirmed using model hindcasts and ship routing charts (WASA, 1995) and a statistical connection between wave height and mean sea level pressure gradients has also been discovered (Bacon and Carter, 1993, Kushnir et al., 1997). Owing to the paucity of in situ data and termination of the measurement programme it is impossible, using these alone, to assess the geographically extent of the increase, to determine the persistence of the trend into the 90s, and to relate its spatial structure to atmospheric/climatic indices. Wave height climatologies derived from satellite altimeter measurements provide full global coverage, and so can be employed to address such issues.

The wave height climate data set used in these studies covers the period 1985-96, with a gap from mid 1989 to mid 1991, and is generated from altimeter data from three satellites, Geosat (1985-89), ERS-1 (1991-96) and TOPEX/Poseidon (1992 to the present). A consistent, quality-controlled dataset covering the period 1985-96 has been generated by separately calibrating each altimeter against wave height measurements from 24 open ocean buoys selected from the US National Data Buoy Center (NDBC) network of buoys, see Cotton and Carter (1994) for details of the calibration and quality control. After consideration of altimeter sampling and wave climate variability issues the best resolution was determined to be given by monthly mean significant wave heights on a 2°latitude by 2° longitude grid.

2.2. Changes between 1985 and 1996 in the North Atlantic

Before calculating interannual variability and identifying any overall trend it is necessary to remove the seasonal signal which is expected to dominate the dataset, especially in mid-latitudes. Monthly mean wave heights were calculated for each 2° box and the seasonal signal was removed using a simple sine/cosine model (for further details see Cotton and Carter (1994)). The seasonal signal explained some 60% of the variance; it is the remaining 40% which is of primary interest here. By carrying out the analysis separately for 1985-89 and 1991-96 it is possible to determine any changes in wave height between the two periods. This is

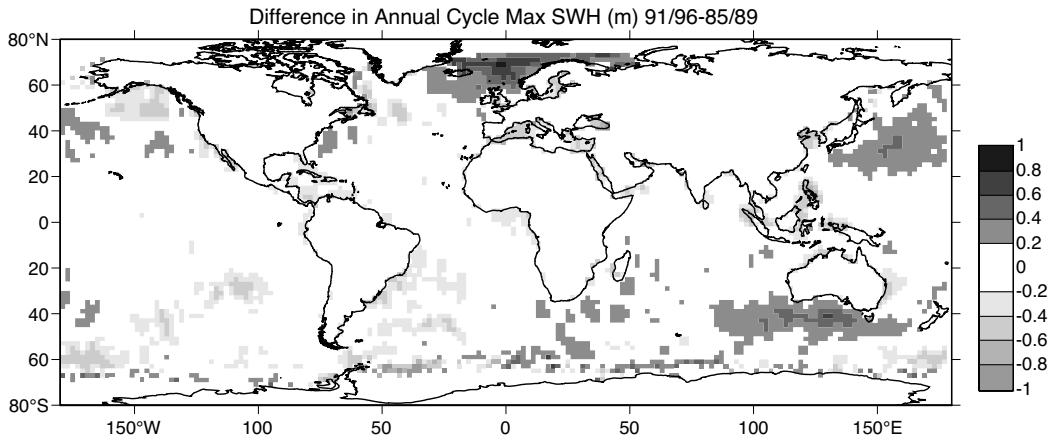

Figure 1. Change in maximum wave height between 1985-89 and 1991-96.

illustrated in Figure 1 in which the change in maximum wave height has been mapped globally. (Away from the tropics these maxima occur during the winter months.) We note that in our area of interest – the North Atlantic – average wave heights were higher in the early 90s than in the late 80s over a large portion of the NE Atlantic. Thus the trend indicated by in situ measurements did continue; moreover the area affected was much larger than was able to be inferred from the surface data. It is interesting to note that this overall increase in wave height from the early 60s until the early 90s parallels the increase in the (smoothed) North Atlantic Oscillation (NAO) Index (Figure 2). The NAO is a measure of the anomaly in the pressure gradient between Portugal and Iceland (see e.g. Hurrell 1995). It is the principal recurrent

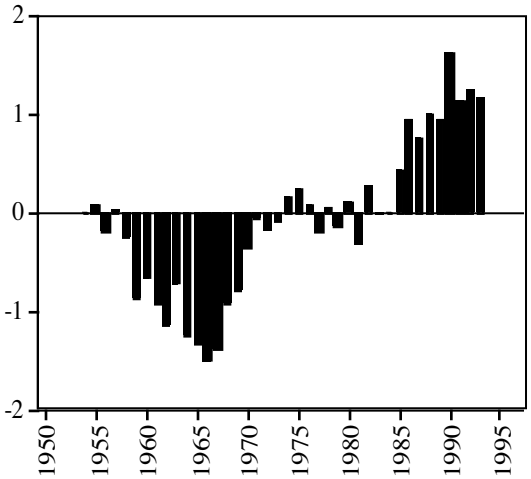

Figure 2. Annual values of NAO Index (9-year running mean).

atmospheric mode in the North Atlantic sector and, recently, has made the largest single contribution to the variability of Northern Hemisphere extratropical temperatures; over the last 3-4 decades it has amplified beyond past experience in a century-long record.

The non-seasonal variability is less easy to characterise than the seasonal cycle. Different "modes" of variability will exhibit different characteristics, a consequence of the various forcing mechanisms. To generate a picture of the spatial structure of this non-seasonal variability, the residual wave height climate data set (i.e. with the annual cycle removed) was analysed using the technique of Empirical Orthogonal Functions (see e.g. Preisendorfer, 1988). Such analysis partitions the signal into different modes ranked by the amount of variance they explain. Examining the most significant modes can reveal interesting patterns of variability. Figure 3 illustrates the spatial structure and time series of the most significant mode, which accounted for 42.2% of the variance in the non-seasonal wave climate variability in the North Atlantic. The Figure shows a bipolar structure which is negative to the south-west and positive to the north-east, the dividing line running south from the southern tip of Greenland and then roughly east towards the Iberian peninsula.

The time series of this first EOF, bottom panel of Figure 3 (solid line), indicates that this pattern increased in strength from the mid 1980s until 1994, after which a weakening occurred. To allow a consideration of how well interannual variations in the pattern of wave climate variability relate to the NAO Index the latter is also shown (dashed line).

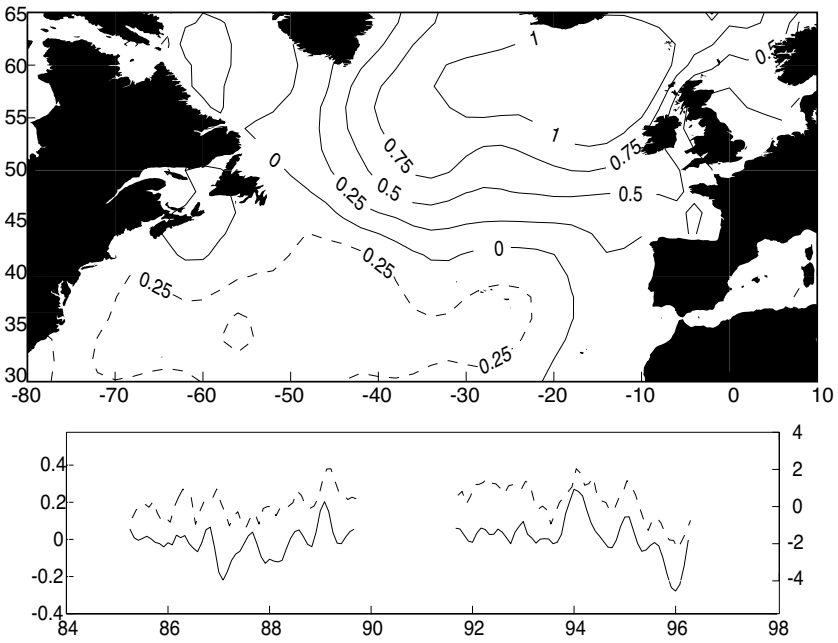

Figure 3. The most significant EOF mode of inter-annual wave climate variability, accounting for 42.2% of variance. Upper Panel: Spatial pattern, contours at 0.25 intervals, dashed lines indicate negative contours, solid lines for positive. Lower Panel: EOF time series (solid line - left hand y-axis), and 5 month running mean North Atlantic Oscillation Index (dashed line - right hand y-axis).

2.3. Connections between North Atlantic and the North Pacific

Although the focus of this paper is the North Atlantic examination by eye of a series of global annual mean wave height maps reveals a marked relationship between two particular

regions, the NE Atlantic and the NE Pacific. To illustrate this we have produced time series of monthly mean wave heights for one 2° box in each region, chosen to be close to the locations of maximum interannual variability (Figure 4). A very obvious inverse relationship is evident which not only raises interesting scientific questions as to what mechanisms are responsible but may be of practical significance, e.g. in carrying out global risk assessments for insurance purposes.

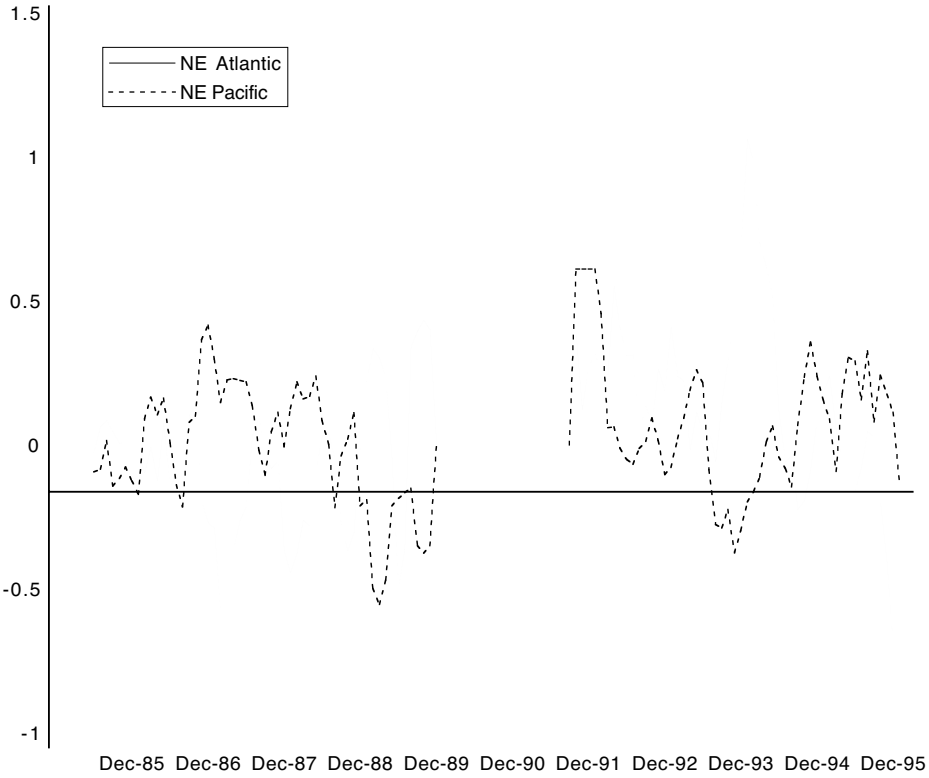

Figure 4. Time series of wave height in 2˚ boxes located in the NE Atlantic (near OWS Lima) and the NE Pacific.

2.4. Future Trends

The significance of the NAO/wave climate correlation identified in Figure 3 suggests the possibility that the NAO could be used as a predictor for the significant part of the non-seasonal wave climate variability. The connection could be used to predict future wave climate, by extracting sea level pressure fields from global circulation models according to the various IPCC scenarios (e.g. double CO_2). This scheme would have the advantage of removing the need to rely on global wave models, which do not yet have a perfect formulation, forced by (necessarily) limited resolution wind fields, a combination which has been shown in the past to underestimate natural climate variability (Sterl et al., 1996). An equally fascinating possibility would be the hindcasting of historical wave fields, based on the estimated NAO values extending back into the 17th century which have been generated from analysis of Greenland ice cores. Clearly such wave forecasts are dependent on good estimates of the NAO.

3. ROSSBY WAVE PROPAGATION

3.1. Background

Rossby waves are a dynamical mechanism for transient adjustment of ocean to changes in large-scale atmospheric forcing and appear as long wavelength features propagating westwards with respect to the mean flow at rather low speeds (typically a few kilometres per day). They are the only way information about events that happened at the eastern boundaries can be transmitted all the way across the oceanic basins and are responsible for westward intensification of large-scale circulation. Because of their low speed and the time they take to cross the oceans, they act as a 'delay line' in the transmission of the effects of climatic events like El Niño. They are associated with changes in sea level, SST and possibly ocean colour.

Because of the spatial (and dynamical) nature of Rossby waves they are difficult to detect in conventional oceanographic measurements such as current meter moorings and hydrographic sections. The radar altimeter, however, is an excellent instrument for studying such phenomena. The first detection of Rossby waves in altimetry was achieved with Geosat data (e.g. Le Traon and Minster, 1993; Tokmakian and Challenor, 1993).

3.2. Methods for calculating propagation speeds

The basis for the detection of Rossby waves in altimeter data is the Hovmöller diagram or longitude/time plot. To construct such a diagram altimeter data are interpolated to a grid and east-west sections are 'stacked' to give a two-dimensional plot whose x-axis is longitude and y-axis is time. The process is illustrated in Figure 5. Westward propagating signals can clearly

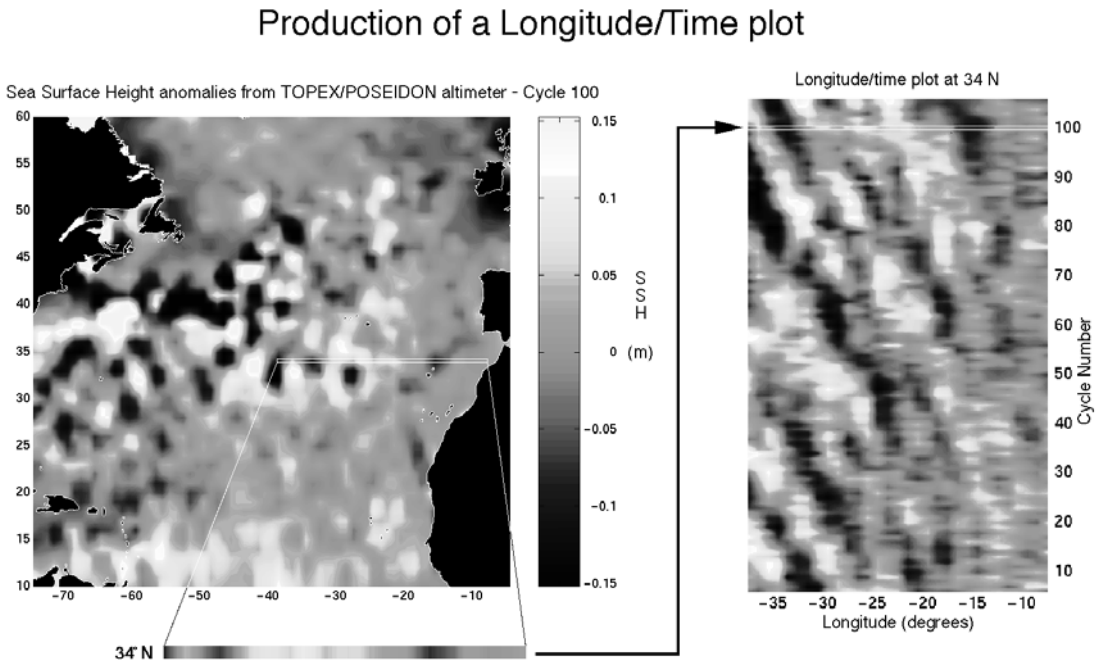

Figure 5. Production of a sea surface height anomaly longitude-time plot, or Hovmöller diagram, at a given latitude (34 °N).

be seen in such diagrams as areas of local maxima and minima running from bottom right to top left across the diagram. The speed of these signals can easily be calculated by hand by simply

taking the slope of the diagonal alignments of maxima and minima. While such a procedure is easy to carry out on a few diagrams, a more automated objective method is required to calculate propagation speeds for entire ocean basins. One possibility is to use Fourier methods, see for example Tokmakian and Challenor (1993) or Cipollini et al. (1997). An alternative is to mathematically define the technique we used by hand. In signal processing such a method is the Radon transform, first described by Radon (1917) in which the orientation of the features on the Hovmöller diagram is obtained by searching for that direction in longitude-time space which maximises the variance and taking the angle orthogonal to that. Rossby wave speeds in the zonal direction are thus relatively easy to calculate using the Radon transform. The method also allows the amplitude of the signal to be estimated.

Although theory predicts that Rossby waves will travel zonally, at least in the absence of topography, in practice we may expect a small northward or southward component to their velocity. The standard two-dimensional Radon transform can be used on a Hovmöller diagram arranged north-south rather than east-west but since we expect the meridional component to be very small or zero this is not very satisfactory. An alternative is to generalise the method into three dimensions in which the dataset is considered as a cube in which the x, y and z axes are longitude, latitude, and time respectively and a search is made for that direction which maximises the variance. Speed can then be calculated from the elevation angle while azimuth angle gives the propagation direction. A choice has to be made as to how many data points are used in each estimation.

3.3. Results for North Atlantic

For the analysis in the North Atlantic we used T/P cycles 1 to 159 (September 1992 to January 1997). The Altimeter Geophysical Data Records from AVISO were processed to retrieve the sea surface height anomalies (SSHAs), which were then gridded cycle by cycle on a 1° by 1° grid. The 3-D Radon transform method outlined above was applied to a 9°x9°x159 cycle sub-domain, which in turn was stepped across the whole dataset in 2°x2° intervals. Figure 6 shows the direction of the predominant propagating signal found and Figure 7 highlights the changes in the speed of the waves for those whose direction of propagation lies within ±20° of 270°.

From Figure 6 we see that there is a well-definite zonal band centered on 33°-34°N where the strongest propagating signal is almost purely westward. The propagation speed in this band (and in other locations in the western part of the basin) is consistent with the speed expected for Rossby waves. This zonal waveguide of stronger Rossby wave propagation just south of the Azores Current had already been observed in T/P data by using standard Fourier and 2-d Radon transform methods (Cipollini et al. 1997, 1999).

When we examine the direction of propagation of the waves in more detail, we see that the topography has no clear effects. It can however be observed that there is a wide mid-latitude zonal band in the North Atlantic (approximately 20°N to 40°N) where the proposed method retrieves a quasi-westward signal (say, within ±10° from pure westward). The propagation speed (Figure 7) increases equatorwards in accordance with the theory, and some effects of topography on speed can be seen, at least in the waveguide from 30° to 36°N, as hypothesized by Tokmakian and Challenor (1993) and theorized by Killworth and Blundell (1999). In this

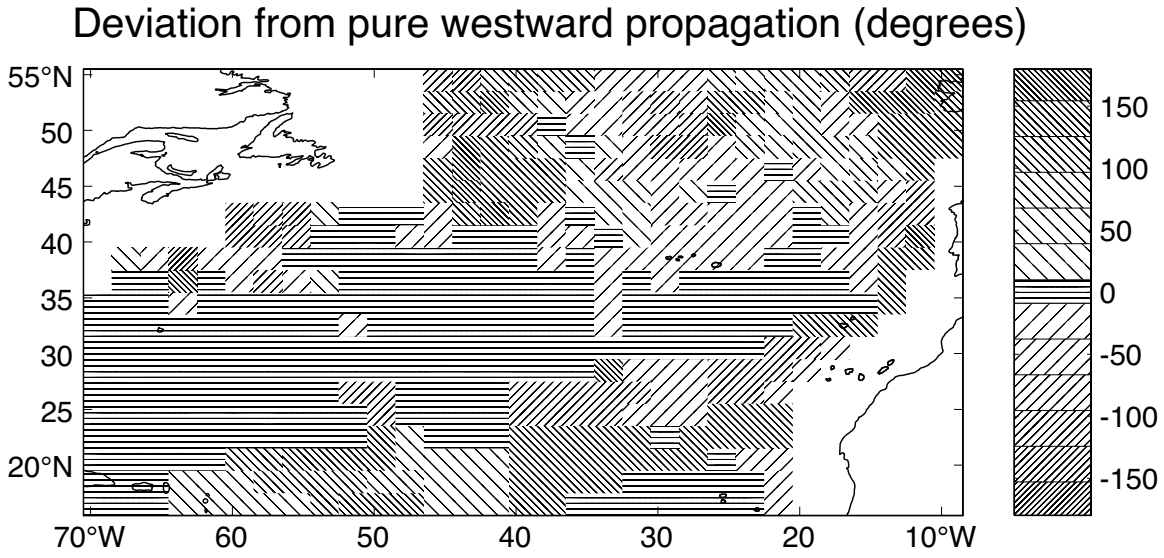

Figure 6. Deviation from pure westward propagation direction in the N Atlantic

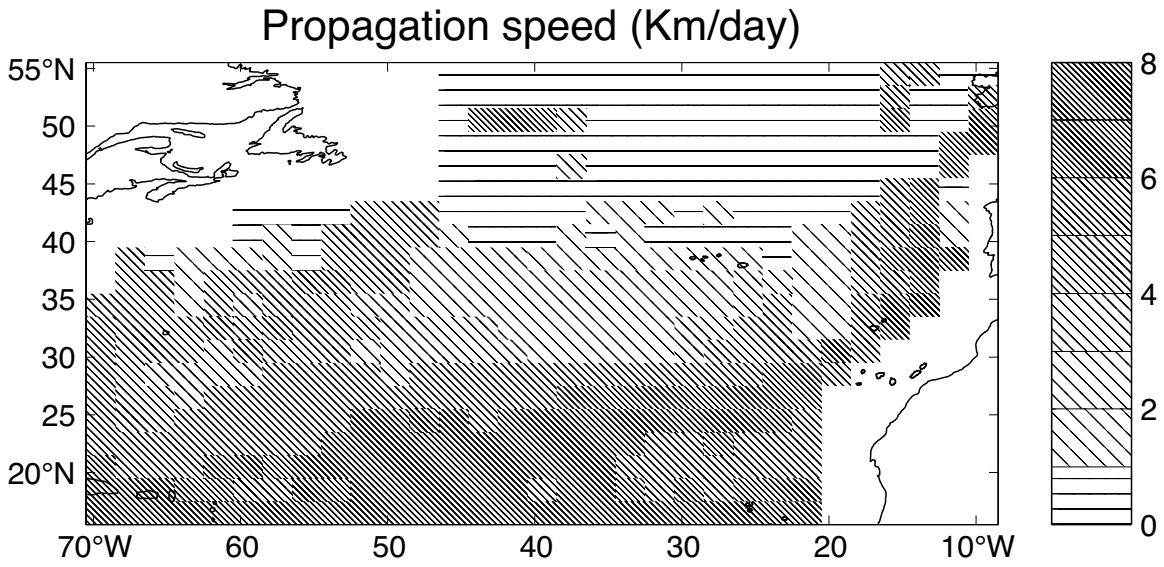

Figure 7. Speed of the main propagating signals (within ±20° of pure westwards).

most energetic waveguide, the waves speed up to 4 km/day once they have past the Madeira Reef and enter the Monaco Basin. Then they slow down on approaching the region of the Plato and Atlantis seamounts at 28°W and subsequently on crossing the Mid-Atlantic Ridge, where their speed has decreased to about 2 km/day. Finally, they speed up again in the western sub-basin. Consistently, we find that these measured propagation speeds

exceed those predicted by the standard theory which assumes the ocean is at rest (Figure 8) but agree rather better when a more realistic ocean is modelled (Killworth et al., 1997).

Rossby waves are also observed in sea surface temperatures measured by the Along Track Scanning Radiometer on ERS-1 and –2. Although features can be seen which propagate with the same speeds as those seen in altimetry the strongest SST signals do not necessarily travel with the same speed as those seen in sea level – possibly because we observe different propagating modes. Such behaviour is consistent with Killworth et al.'s theory. Very recently, we have analysed ocean colour data from the OCTS on ADEOS and from SeaWiFS and this also suggests the presence of Rossby waves which opens up exciting possibilities for predicting modulations in biological activity.

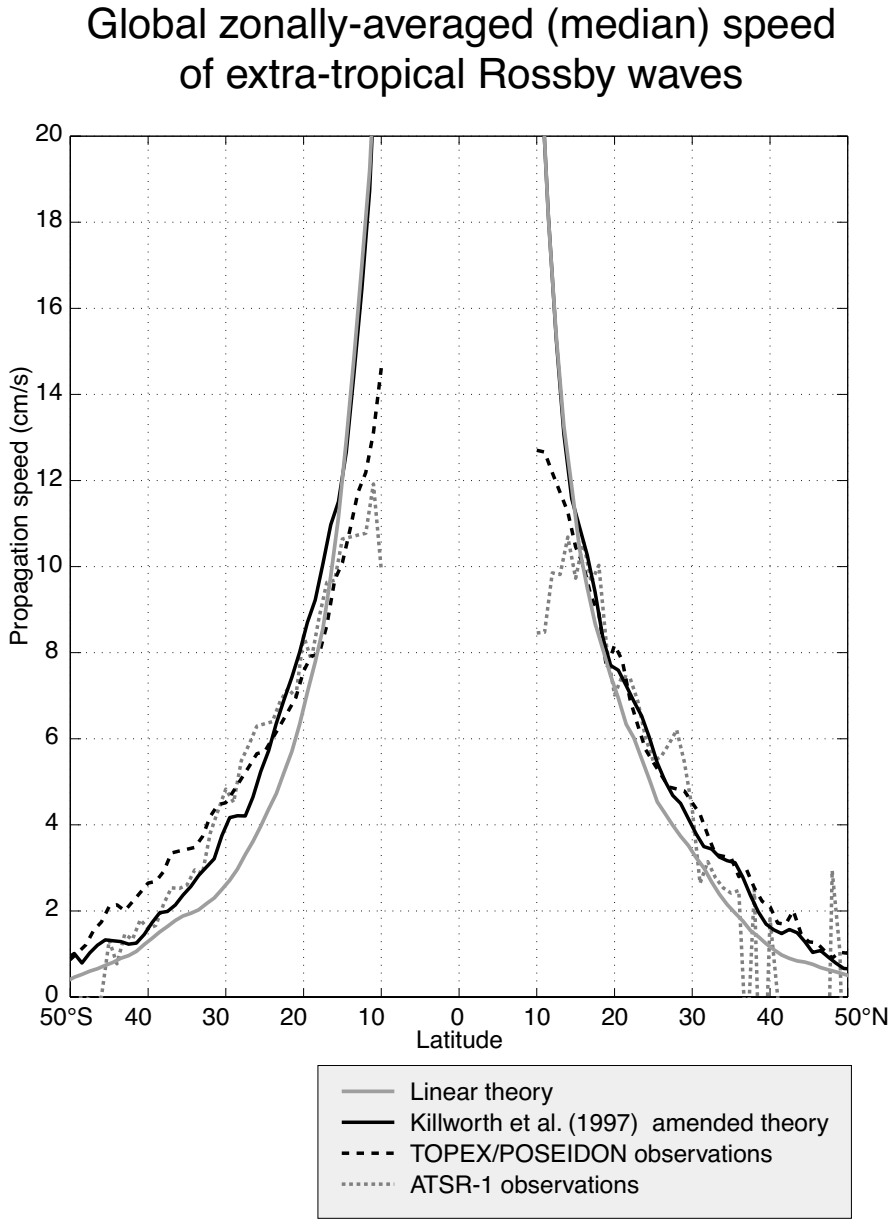

Figure 8. Comparison of observed propagation speeds with theoretical values assuming the ocean is at rest.

4. A NEW PRECIPITATION CLIMATOLOGY

4.1. Background

Precipitation at sea has been identified as one of the parameters required by EuroGOOS. It affects near surface salinity and, together with evaporation, plays a significant role in the thermohaline circulation and hence in climate. Information concerning oceanic rainfall is also clearly important in understanding the dynamics of the global atmosphere. However, measuring global precipitation to useful accuracy has been a task challenging sensor developers for some time. It is difficult to observe by ship, owing to flow distortion by the ship's superstructure, and also the understandable tendency of ships to avoid known storms. Additionally, some ocean regions, particularly the Southern Ocean, are poorly sampled by ships or buoys. The range of land-based rain radars is a few hundred kilometres, and sampling by low-flying research aircraft is sporadic. As rain varies rapidly on both spatial and temporal scales, this is a field where only satellite-based measurements have the potential for achieving the coverage desired. However, care must be taken in deriving precipitation estimates as bias can be present if the local sampling time is always the same, due to diurnal effects (this is not a problem for the altimeter estimates discussed in the next section; see Quartly et al., 1999).

A number of spaceborne sensors, using visible, IR, active and passive microwave techniques, have exhibited sensitivity to rain, or to other features associated with rain; however, only one to-date has had the measurement of rainfall as its principal goal. This satellite called TRMM (Tropical Rainfall Measuring Mission) was launched in November 1997 and provides good resolution and coverage but is limited to latitudes between 35˚S and 35˚N. Global rain rates can be calculated from SSM/I, but these need adjustment for the large footprint of the instrument.

4.2. Basis of a new altimeter climatology

Recently, a technique has been developed by Quartly et al. (1996) for the estimation of rain within an altimeter footprint. The approach makes use of the fact that the radar backscatter at K_u-band radar frequencies is significantly attenuated by rain whereas radar pulses at C-band are hardly affected. By applying the method to the dual-frequency TOPEX altimeter we have been able to calculate rain-rate using a simple physically-based algorithm (Quartly et al., 1999). In order to convert attenuation to rain-rate an assumption has to be made concerning the vertical extent of the rain column, *H*. Here, as in Quartly et al. (1999) we have taken *H* to be 5 km everywhere. This is a reasonable value for the tropics but not for mid-latitudes and so it is expected that the rain-rate algorithm might lead to underestimates outside the tropics. To make allowance for the particular sampling of a single altimeter we bin the data in boxes 5˚ in longitude by 2.5˚ in latitude and for a duration of 2 months. These values reduce the sampling error to the order of 15-20%, according to the frequency of occurrence of rain. As TOPEX is not in a sun-synchronous orbit, there is no diurnal bias in 2-month averages.

4.3. General features

Using the data from each lat/long box an analysis of all the 2-month periods extending from January-February 1993 to September-October 1998 was carried out. Figure 9 shows an example of the global distribution of inferred rain-rate, for one of the two-month periods, March-April 1994. An inspection of all such plots indicates that this is typical. The distribution of the higher values corresponds very well to the known climatological rain zones,

e.g. the Inter-Tropical Convergence Zone (ITCZ), the South Pacific Convergence Zone (SPCZ) and the mid-latitudes, especially on the western side of ocean basins. Monthly accumulations range from more than 200 mm in the tropics to between 100 and 200 mm in mid-latitudes.

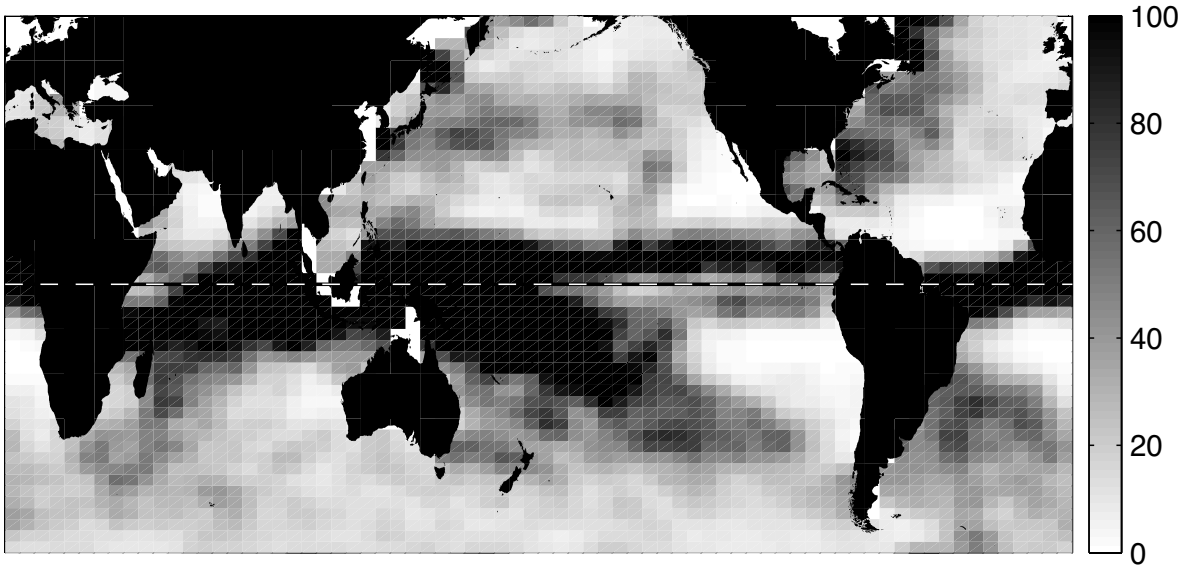

Figure 9. Global rain-rate distribution (mm/month), March-April 1994.

4.4. Changes associated with the El Niño

From an examination of of all the 2-month plots the most striking changes occur during the latter half of 1997 and the first half of 1998 when a major El Niño is known to have occurred. To highlight its manifestation in rainfall we have computed anomalies with respect to biomonthly means for 1993-96. As this was a period with small values of the Southern Oscillation Index it implies that there was no strong El Niño (or La Niña).

The anomalies for March 97 – August 98 are shown in Figure 10. From May 1997 onwards an area of high anomaly moved eastwards across the Pacific such that by March-April 1998 a positive anomaly exceeding 50mm/month was located in the E. Pacific with a negative anomaly of more than 50mm/month in the far west. This is a good example of the eastwards shift of the main precipitation region during an El Niño. The broad E-W band of high anomalies across the Pacific lying just to the south of a band of low anomalies was also a marked feature and can be interpreted as a southwards shift of the ITCZ. Quartly et al. (2000) show that during the "El Niño period" not only is there a southward migration of the ITCZ, but also it becomes broader, with more frequent occurrences of rain. During the same period there were coherent changes in the Indian Ocean. In the second half of 97 anomalously high rainfall occurred in the northwest and anomalously low in the east. Gradually, in 1998 the high anomaly moved east towards Indonesia.

We have also examined the North Atlantic during the same period (Figure 11), again using anomalies referenced to 1993-96. The whole period appears to be characterized by transient anomalies with no readily identifiable persistent feature that can be associated with the El Niño. However, in the tropics throughout most of 1997 there are adjacent bands of high and

low anomaly which could be interpreted as a northward displacement of the ITCZ. Outside the tropics precipitation appears to be higher in the central North Atlantic in 1998 than 1997.

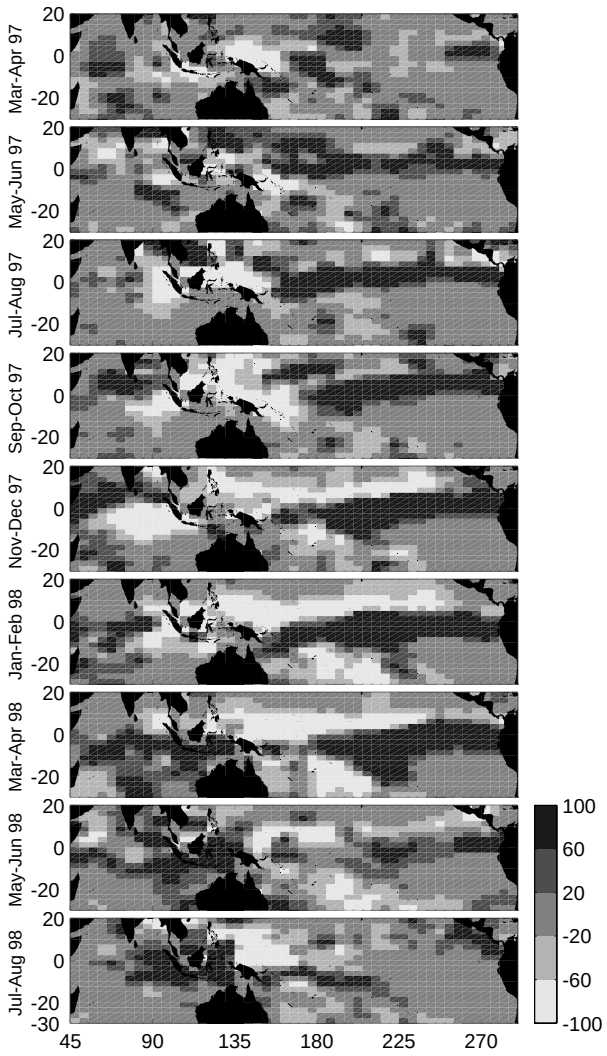

Figure 10. Tropical Pacific rain-rate anomalies (mm/month) for March-April 1997 – July-August 1998, referred to the relevant 2-month means for 1993-96.

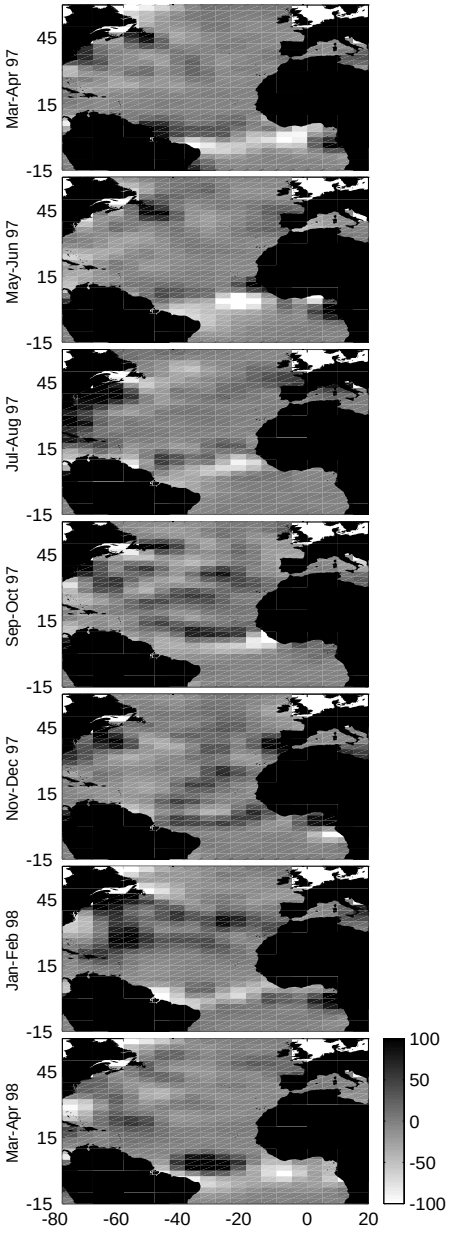

Figure 11. As Figure 10 but for the Atlantic north of 15˚ S.

4.5. Time series of basin-scale means

In order to provide further insights into our new climatology, we have calculated mean rainfall rates for different basins – tropical and extra-tropical North Atlantic, tropical Pacific and the Indian Ocean north of the equator. Tropical here is taken to be within ±15˚ of the

equator. Figure 12 shows the temporal variation of these quantities for the period January 1993 – October 1998. There are several features to which we draw attention:

(a) Mean rainfall is higher in the tropical Pacific and Indian Oceans than in the tropical Atlantic
(b) The Indian Ocean has the highest seasonal signal
(c) The overall amount of rainfall increases with the onset of the El Niño in both the tropical Pacific and in the Indian Ocean
(d) In January-February, some two months before the El Niño is generally regarded to have developed the North Indian Ocean rainfall reached its lowest value in the 6-year period. Whether this precursive behaviour is present in other El Niños is not known.
(e) There is no clear El Niño signal in the tropical Atlantic; the meridional displacement of the ITCZ referred to above does not show up because it does not extend beyond ±15˚.

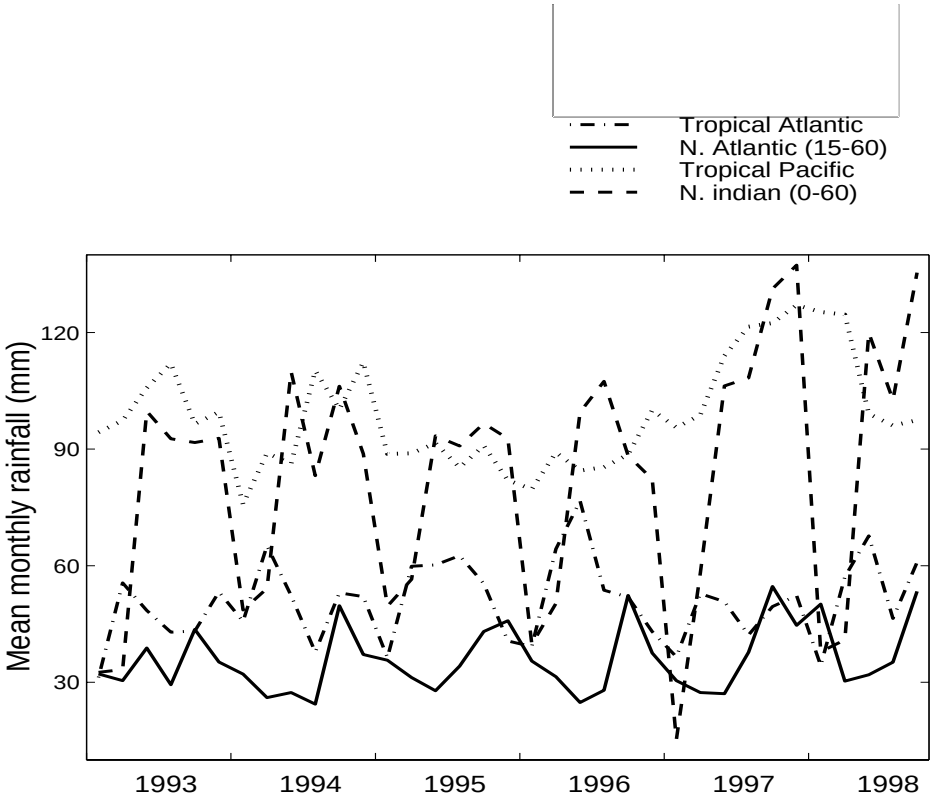

Figure 12. Time series of mean monthly rain rates in four ocean areas (see text for further details)

4.6. Relationship to other climatologies

At present our values in the tropics are about 75% of those in the GPCP climatology (Huffman et al., 1997) for the same period. However given that a study of infra-red- and SSM/I-derived rain rates in the TOGA COARE region showed them to be typically 30% high (Ebert and Manton, 1998), we do not feel it would be wise to adjust our values towards a closer comparison with other satellite-derived climatologies. Our derived values for the mid-latitude bands may need multiplying by a factor of about 1.5 to correct for the assumption that

H is constant with latitude. We are confident that our TOPEX-derived values can make a useful contribution to global precipitation climatologies, and with two further dual-frequency altimeters to be launched soon — *JASON-1* and *Envisat* — a long time record of such measurements is envisaged. As long as sufficiently long time and spatial averaging is used, the uncertainties in deriving precipitation climatologies from altimetry appear comparable with those from other satellite remote sensing techniques.

5. CONCLUDING REMARKS

This paper has summarised recent work at SOC and demonstrates that satellites are able to routinely monitor wave height, Rossby waves, and precipitation on different scales over the world ocean. To do this it is important to have both continuity of, and consistency between, satellite missions as exemplified by the changes in wave height deduced from 3 successive altimetric satellites. Although the altimeter is remarkable for its diversity of applications its very narrow swath can lead to unacceptable sampling errors, especially for short time scales. A constellation of altimeters such as proposed for GANDER would improve the situation significantly for both wave climate and, provided they are dual frequency, for precipitation. Precise orbit determination is not a requirement for these applications. The measurements described in this paper can be used not only for monitoring but, through assimilation into models, for improved simulation and forecasting. They are also useful for model validation. Although our studies were carried out using off-line data for forecasting purposes there is a need to obtain the processed data in near real-time. Thus, the delivery-time requirement depends on the application.

REFERENCES

Bacon S. and D. J. T. Carter, 1991. Wave climate changes in the North Atlantic and North Sea, *Int J. Climatol.*, 11, 545-558.

Bacon S. and D. J. T. Carter, 1993. A connection between mean wave height and atmospheric pressure gradient in the North Atlantic, *Int J. Climatol.*, 13, 423-436.

Cipollini, P., D. Cromwell, M. S. Jones, G. D. Quartly and P. G. Challenor, 1997. Concurrent TOPEX/POSEIDON altimeter and Along-Track Scanning Radiometer observations of Rossby wave propagation near 34^{o}N in the Northeast Atlantic, *Geophys. Res. Letters*, 24, 889-892.

Cipollini, P., D. Cromwell and G. D. Quartly, 1999. Observations of Rossby Wave propagation in the Northeast Atlantic with TOPEX/POSEIDON altimetry, *Adv. Space Res.*, 22, 11, 1553-1556.

Cotton, P. D. and D.J.T. Carter, 1994. Cross calibration of TOPEX, ERS-1 and Geosat wave heights. *J. Geophys Res.*, 99, C12, 25025-25033.

Ebert, E.E., and M.J. Manton, 1998. Performance of satellite rainfall estimation algorithms during TOGA COARE, *J. Atmos. Sci.*, 55, 1537-1557.

Huffman, G.J., R.F. Adler, P. Arkin, A. Chang, R. Ferraro, A. Gruber, J. Janowiak, A. McNab, B. Rudolf, and U. Schneider, 1997 The Global Precipitation Climatology Project (GPCP) combined precipitation dataset, *Bull. Am. Met. Soc.*, 78, 5-20.

Hurrell, J. W., 1995. Decadal trends in the North Atlantic Oscillation: Regional temperatures and precipitation, *Science*, 269, 676-679.

Killworth, P. D., D. B. Chelton and R. deSzoeke, 1997. The speed of observed and theoretical long extra-tropical planetary waves, *J. Phys. Oceanogr.*, 27, 1946-1966.

Killworth, P. D. and J. R. Blundell, 1999. The effect of bottom topography on the speed of long extra-tropical planetary waves. *J. Phys. Oceanogr.*, 29, 2689-2710.

Kushnir Y., V.J. Cardone, J.G. Greenwood and M.A. Cane, 1997. The recent increase in North Atlantic wave heights, *J. Clim.*, 10, 2107-2113.

Le Traon, P.-Y. and J.-F. Minster, 1993. Sea Level Variability and Semiannual Rossby Waves in the South Atlantic Subtropical Gyre, *J. Geophys. Res.*, 98, 12,315-12,326.

Preisendorfer, R., 1988, *Principal Component Analysis in Meteorology and Oceanography,* Elsevier Pub. Co., N.Y.

Quartly, G.D., T.H. Guymer, and M.A. Srokosz, 1996. The effects of rain on TOPEX radar altimeter data, *J. Atmos. Oceanic Technol.*, 13, 1209-1229.

Quartly, G.D., M.A. Srokosz, T.H. Guymer, 1999. Global Precipitation Statistics from Dual-Frequency TOPEX Altimetry, *J. Geophys. Res.*, 104, 31,489 – 31,516.

Quartly, G.D., M.A. Srokosz, T.H. Guymer, 2000. Changes in oceanic precipitation during the 1997-98 El Niño, *Geophys. Res. Lett.*, 27, 2293 – 2296.

Radon, J., 1917. Über die Bestimmung von Funktionen durch ihre Integralwerte längs gewisser Mannigfaltigkeiten, *Berichte Sächsische Akademie der Wissenschaften. Leipzig, Math.–Phys. Kl.*, 69, 262-267. English translation in S.R. Deans, 1983, *The Radon transform and some of its applications*: John Wiley, pp. 204-217.

Sterl, A., G.J. Komen and P.D. Cotton, 1998. 15 years of global wave hindcasts using ERA winds: validating the reanalysed winds and assessing the wave climate, *J. Geophys. Res.*, 103, C3, 5477-5492.

Tokmakian, R. T. and P. G. Challenor, 1993. Observations in the Canary Basin and the Azores Frontal Region Using Geosat Data, *J. Geophys. Res.*, *98*, 4761-4773.

WASA group, 1995. The WASA project: Changing storm and wave climate in the North-East Atlantic and adjacent seas? *Proc. fourth international workshop on wave hindcasting and forecasting*, Banff, Canada October 16-20.